# Predication of Planar Near-Field Measurements Based on Full-Wave Three-Dimensional CEM Measurement Simulation

R. F. Dubrovka[1],
R.C. Jones[1], C.G. Parini[1].
[1]School of Electronic Engineering and Computer Sciences
Queen Mary University of London
London, E1 4NS, UK
r.dubrovka@qmul.ac.uk

S.F. Gregson[1,2], *Fellow, AMTA.*
[2]Next Phase Measurements
CA, USA
stuart.gregson@npmeas.com

***Abstract*—In this paper, the full-wave computational electromagnetic simulation of the production test, measurement, and calibration of a 5G, 24 elements, C-band, active, planar array antenna together with a representative open-ended rectangular waveguide probe with, and without, absorber collar were evaluated using a large computing cluster and a proprietary full-wave solver. In this way, various components within the measurement could be carefully and precisely examined providing a framework for further measurement optimization. Particular attention has been paid to the presence of the standing waves in the simulated near-field measurement. This is a crucial feature of most practical measurements, but is omitted from the vast majority of simulations due to the computational effort required to evaluate it, and which is absent from the standard near-field theory. Here, the presence and impact of this phenomenon has been carefully examined with a range of intensive simulations being harnessed to quantify their impact, as well as enabling various methods for their minimization to be explored in a convenient and highly controlled fashion.**

## I. INTRODUCTION

In recent years, Model Based Systems Engineering and Development (MBSE/MBD) approaches have found great utility in dramatically reducing the amount of time, effort, and cost needed for the programme development and validation required by many modern complex antenna testing projects [1]. This trend has been made possible by the rapid growth in power of modern computational facilities which have only comparatively recently enabled the full-wave three-dimensional computational electromagnetic (CEM) simulations to emulate realistic empirical free-field measurements. Thus, MBSE tools can now be used to optimize measurement configurations, to evaluate and reduce measurement uncertainties, to verify and validate processing techniques [1, 2], as well as to develop and refine new concepts of operation (ConOps) early on within the project cycle [3].

The paper structure is as follows. After Introduction, the second section describes numerical models and a "measurement" setup. In the third section results of planar near-field measurements of the AUT are presented. Section IV is dedicated to investigation of standing waves and probe compensation, offering a much better and deeper insight to the planar near-field measurements. The paper finishes with the Conclusions.

## II. PREPARING THE FULL 3-D ELECTROMAGNETIC MODEL

In order to undertake any simulation, a model of the desired setup has to be created. In the presented paper, it is a model which emulates a real antenna measurement setup. The model obviously should consist of two basic elements. One is an antenna under the test (AUT) and the other is a probe antenna, which will be called "the probe" further in the text for sake of simplicity.

A finite antenna array has been chosen as an AUT. The AUT consists of 48 patches in a 6 x 8 array and is shown in Fig. 1. Overall dimensions of the AUT are 200 by 300 mm, operating at 3.5 GHz. To avoid extra complexity of simulations, all elements are pin fed with equal magnitudes and phases, and their feeding networks are represented as an ideal circuit which is excluded from the discussion here.

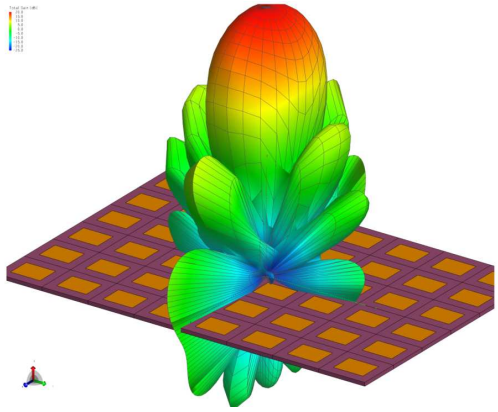

Figure 1. Antenna under test (AUT) shown with far-field antenna pattern

An open-ended rectangular waveguide (OEWG) probe has been selected to perform as a probe in the numerical measurements experiment. An overall view of the probe is demonstrated in Fig. 2, which is a standard C-band waveguide

section probe fed by a coaxial-to waveguide adaptor. The dimensions are as follows: waveguide width = 47.55mm; waveguide height = 22.15mm; wall thickness = 1.59mm; coaxial pin length = 11.08mm; coaxial used – RG141U. The inclusion of the coax-to-waveguide transition is important as terminating the waveguide section with a perfect WG port would provide an overly optimistic estimation of the scattering characteristics of the near-field probe.

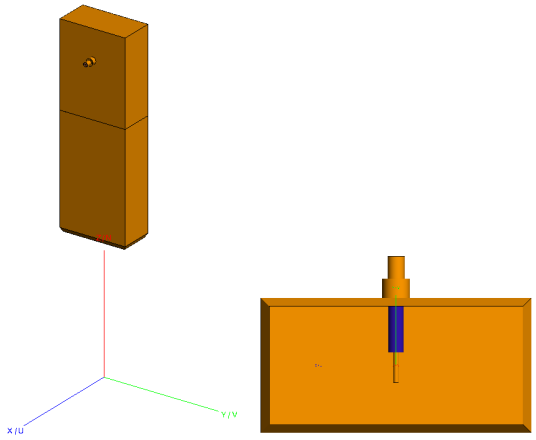

Figure 2. View of OEWG near-field probe, right hand side showing coax-to-waveguide transition.

A model of the "measurement system" has been created and simulated in the full-wave three-dimensional computational electromagnetic (CEM) solver Altair FEKO [4]. The choice of the software has been dictated by the intrinsic hybrid nature of the CEM package which allows for omission of the free space meshing between the AUT and the probe. The MoM/MLFMM solver has been utilised as a solution to this problem.

## III. Near-field studies of the AUT

First of all, a full 2-D map of near-field distributions in planes parallel to the AUT surface were obtained via the CEM solver of the stand-alone AUT. It is an important step to have a benchmark which can be used to compare true and "measured" results. Here and below, results of our full-wave numerical simulations of the planar NF process referred to as "measurements" or "measured". The complete NF measurement setup is shown in Fig. 3, with the NF measurement plane taken at a distance of 460 mm which is approximately five wavelengths, a fairly typical AUT-to-probe separation that could be used in a practical measurement, and which is large enough to insure reactive, evanescent, fields are well attenuated and absent from the simulated measurement.

For the sake of simplicity only the setup with the pyramidal absorber collar is shown in the figure. However, two scenarios have been investigated, namely: with and without the absorber collar. Results for both scenarios will be demonstrated herein below. Also, a thorough investigation of a collar influence on the predicted results have been performed. The absorber collar is an essential part of a near-field probe. It attempts to obscure the mechanical fixtures that are used to support and attach the probe to the near-field positioning equipment and attempts to make the probe radiation pattern somewhat independent of what the probe it is mounted to.

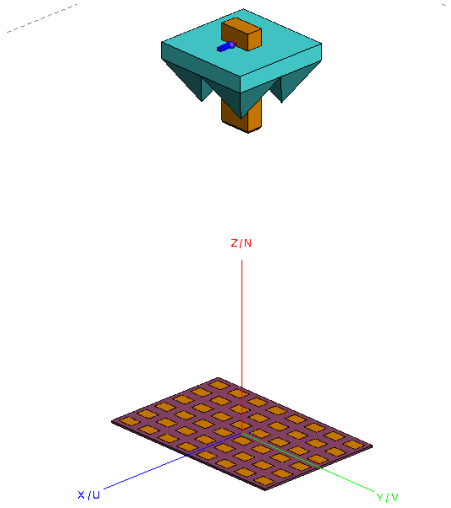


Figure 3. The measurement setup where the probe is in front of the AUT at the distance 460mm.

This is very important as it serves to insure that the probe pattern calibration is valid and differences between the positioning equipment do not unduly influence the radiation patterns. Here, the absorber characteristics were taken from the open literature [5] and is approximated by a material with a dielectric constant of 1.95, and a loss tangent of 0.718. However, details of the absorber modelling is beyond the scope of this paper and will be reported in a separate publication.

The true NF distribution over a planar surface of dimension 2m x 2m is shown in Fig. 4, this size offering valid prediction of the FF pattern out to angles of *circa* 60° [6]. The sampling step in both directions is 40mm which is slightly less than $\lambda/2$ at the operating frequency of 3.5 GHz. The results are computed for only one quadrant due to a full symmetry of the AUT along x- and y-axes and results replicated for the other three quadrants to show the complete NF.

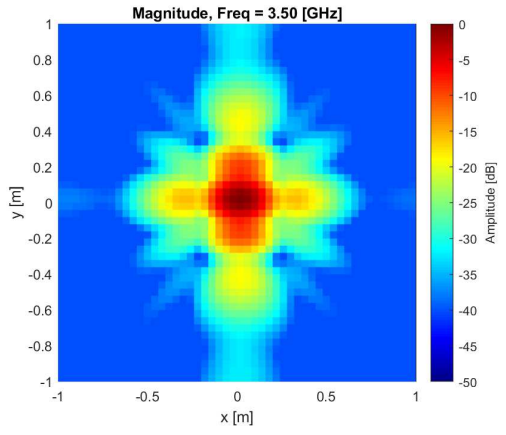


Figure 4. True NF in front of the AUT at the distance 460mm.

The next step is to "measure" a near-field distribution using the probe. In the same plane, at 460mm, a sampling has been undertaken by placing the aperture of the probe in the same positions as in the 'true' simulations of Fig 4. Fig. 5 demonstrates the 'measurement' for the OEWG probe without, top, and with, bottom, the absorber collar. For both scenarios, a measured result is not an electrical field distribution, however, it is a scattering transmission parameter $S_{21}$. In this case, the parameter describes the transmission between the common port which feeds the AUT and the coaxial port at the throat of the OEWG probe. Hence, this simulation replicates a real-life scenario where a NF scanner measures the scattering parameters between two ports of a vector network analyser (VNA) where those ports are connected to the probe and the AUT respectively. Thus, each point in the "measured" near-field corresponds to one complete full-wave three-dimensional electromagnetic simulation. This also corresponds to the most complete and general simulation of the near-field measurement and clearly includes both scattering and transmission effects.

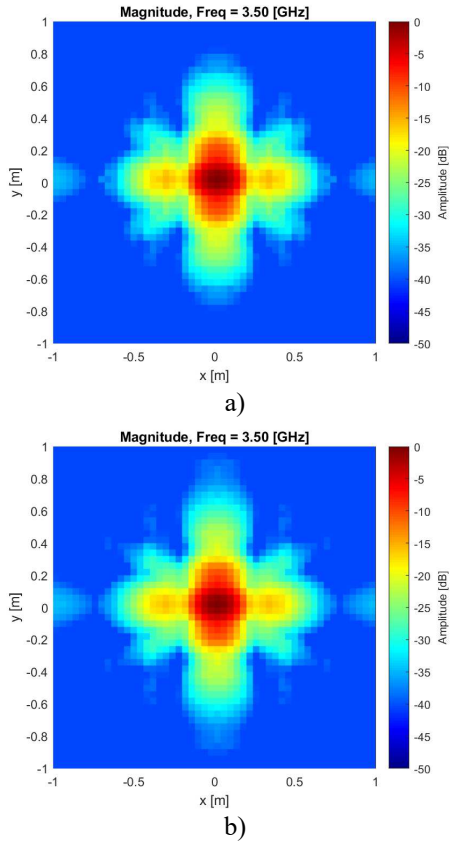


Figure 5. Simulated "measured" NF in front of the AUT at the distance 460mm: a) without the absorber collar; b) with the absorber collar.

A comparison between the true and 'measured' NF is demonstrated in Fig. 6. For more clarity, only the central part of the NF has been shown. It is easily observable that there is some difference between the two results. However, they are very simply explainable, see, for example, [6,7]. Any probe has its own unique radiation pattern and, unlike in the case of a Hertzian dipole, which is used to characterise 'ideal' NF measurements, the probe influences, through its radiation pattern, the field measured at each NF point. It is only after the NF to FF transformation process with probe compensation (which employs a full knowledge of the probes radiation characteristics) that the true FF pattern can be recovered. In addition to the probe's radiation pattern, mutual coupling between the AUT and the probe can exist but this is minimised with a probe to AUT separation of *circa* 3λ or more. Reflections between the probe and the AUT which lead to standing waves existing between them also corrupt the measured NF values and are not compensated within the transformation post-processing.

In Fig. 7 we show the co-polar and cross-polar radiation patterns of the OEWG probe with and without the absorber collar computed using the CEM solver. Clear differences exist which indicate that using the correct Probe radiation pattern is important if the NF to FF transformation with probe compensation is to work correctly.

Before moving to the next section we provide some information on the computer resource required for the modelling process. A simulation of one sampling position in the afore presented scenario, using the 10 CPU core Dell Precision Workstation with 64 GB RAM, takes 3.0-3.5 minutes. The same point can be simulated almost 1.5 times faster utilising a server PC with 512 GB RAM, 32 CPU cores running at 2.2 GHz, and 64 logical processors. However, the number of cores utilised by the simulation is in practice limited to approximately half of those available, as the server is shared and has limitations for a single user. Therefore, a single frequency run over one quadrant of the AUT, consumes from 20 to 30 hours of a high-performance workstation.

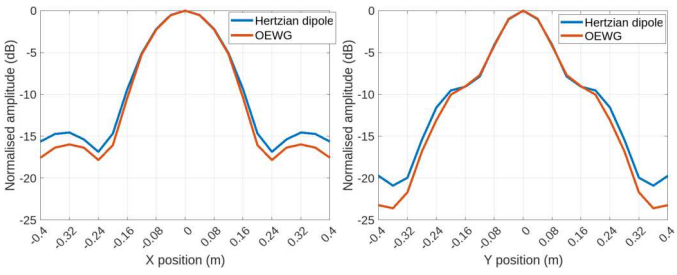


Figure 6. Comparison of the two simulations: a) E-field distribution along the x-axis; b) E-field distribution along the y-axis.

## IV. Standing Wave Investigation and Probe Compensation

As mentioned in the previous section, results of measurements can be affected by the choice of longitudinal position of the probe. Due to the computational effort required, relatively little attention has been paid to this in the open literature, and although in general near-field range assessments do attempt to estimate the AUT-to-probe multiple reflections uncertainty term experimentally [10], this is the first time this has been attempted numerically. Thus, in this section, results of

such investigations are presented and discussed. Furthermore, the second part of the section demonstrates how use of probe compensation allows for almost perfect measurement results comparing to theoretical field distribution obtained without any probe influence.

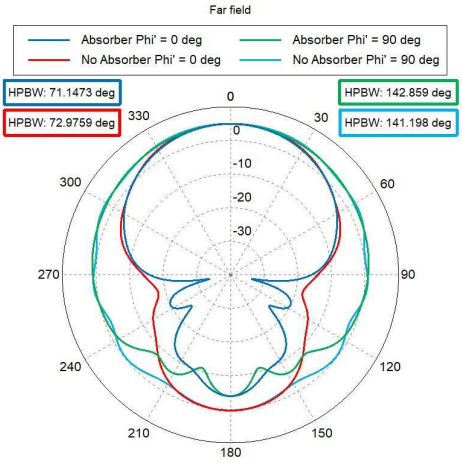


a)

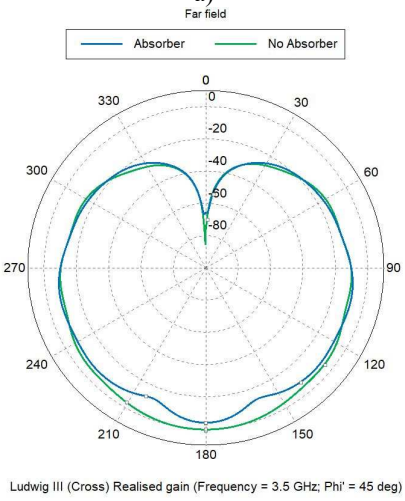


b)

Fig7. OEWG probe radiation patterns with and without absorber collar: a) co-polar; b) cross-polar.

To commence this investigation a new set of numerical measurements has been performed. These consist of a linear scan along the z-axis, *i.e.*, perpendicular to the AUT aperture plane and in line with the centre of the array. Results of such measurements for both cases, with and without the probe absorber collar are compared in Fig. 8. Clearly there are ripples on both plots resulting from multiple reflections between the AUT and the probe. It is demonstrated that the inclusion of the absorber collar has not unduly upset the near-field measurement. Moreover, the level of ripple relative to the Hertzian dipole probe for the case with absorber collar, is 0.2dB beyond a separation of 3λ (a typical measurement range length). A NF probe always needs an absorber collar to shield the metal mounting structure of the probe robotic scanner from the incoming AUT field. It can be well justified that the absorber collar is the most important piece of absorber in the whole NF measurement setup [8].

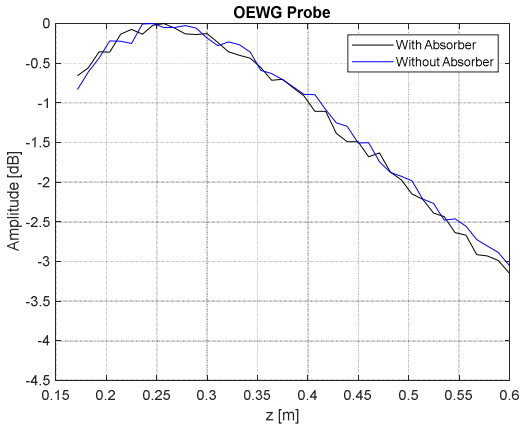


Figure 8. A comparison between two measurement scenarios along z-axis AUT-to-probe separation of 2λ to 7λ.

Finally, in Fig 9 we take the 'measured' NF for the case with the OEWG with absorber collar and undertake the NF to FF transform using probe compensation algorithms [6], and compare to the case for the (true) Hertzian dipole probe. The results show an excellent agreement. The differences we see are an artefact of:

- Differences in the Gibbs ripple [9] of the two NF data sets (infinitesimal probe and OEWG probe),
- AUT-to-probe multiple-reflections.

The presented results demonstrate less oscillations and much smoother dependence for the AUT-probe case. In the main lobe angular space, there is no visible difference in magnitude. However, phase, as a more sensitive parameter, shows visible difference. The farer an observer moves from the main lobe, the disagreement becomes more significant.

## V. CONCLUSIONS

In this paper, full-wave three-dimensional computational electromagnetic simulations of the C-band antenna array measurements have been presented. A very good agreement between true and 'measured' FF results have been demonstrated. The importance of an absorber collar for the OEWG probe has been shown and the level of ripple resulting from reflections between the AUT and probe have been quantified. This paper reports preliminary work concerning the search for the best performing NF probe and offers a baseline for the commonly used OEWG to which other probes can be compared.

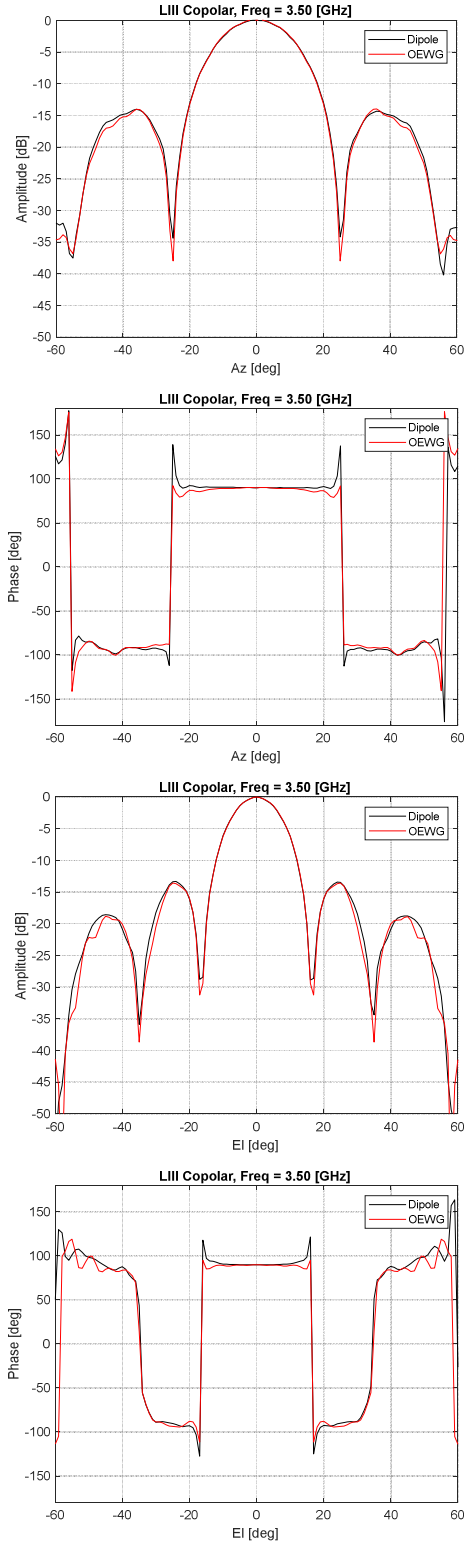


Figure 9. Comparison between two far-field "measurements" using Hertzian dipole and OEWG probe in two principal planes ("Az" stands for azimuth angles and "El" – for elevation angles respectively)

## References


[1] J.A. Estefan, "Survey of model-based systems engineering (MBSE) methodologies.", Incose MBSE Focus Group 25 (2007)

[2] M. Grieves, "Digital Twin: Manufacturing Excellence through Virtual Factory Replication", 2015.

[3] D.M. Lewis, J. Bommer, G.E. Hindman, S.F. Gregson, "Traditional to modern antenna test environments: The impact of robotics and computational electromagnetic simulation on modern antenna measurements," 15th European Conference on Antennas and Propagation (EuCAP), 2021

[4] https://altair.com/feko-applications, accessed on 20th of July, 2023

[5] D. Campbell, G. Gampala, C. J. Reddy, M. Winebrand, and J. Aubin, "Modeling and Analysis of Anechoic Chamber Using CEM Tools," ACES Journal, Vol. 28, No.9, pp. 755-762, September 2013

[6] S. Gregson, J. McCormick, C. Parini, " Principles of Planar Near-Field Antenna Measurements", Second Edition, July 2023, IET Publishing, ISBN-13: 978-1-83953-699-1.

[7] C. G. Parini, R. Dubrovka, and S. F. Gregson, "Computational Electromagnetic Modelling of Compact Antenna Test Range Quiet Zone Probing," ACES Journal, Vol. 33, No. 2, pp.127-131, February 2018.

[8] A Newell, S Gregson, D Gentle, P Miller, "The effect of the absorber collar on open-ended waveguide probes", Antenna Measurement Techniques Association (AMTA), Salt Lake City, Utah, USA, 2009.

[9] Vretblad, Anders (2000), Fourier Analysis and its Applications, Graduate Texts in Mathematics, vol. 223, New York: Springer Publishing, p. 93, ISBN 978-0-387-00836-3

[10] Clive Parini, Stuart Gregson, John McCormick, Daniël Janse van Rensburg and Thomas Eibert, "Theory And Practice of Modern Antenna Range Measurements 2nd Expanded Edition", Volume 1 & 2, IET Electromagnetic Waves series 55, ISBN 978-1-83953-126-2 & ISBN 978-1-83953-128.